Numerical Study of Laminar Core-Annular Flow in a Torus and in a 90° Pipe Bend

Gijs Ooms, Mathieu J. B. M. Pourquie, and Jerry Westerweel
J.M. Burgerscentrum, Delft University of Technology, Faculty of Mechanical Engineering, Laboratory for Aero- and Hydrodynamics, Mekelweg 2, 2628 CD Delft, The Netherlands

DOI 10.1002/aic.14796
Published online March 31, 2015 in Wiley Online Library (wileyonlinelibrary.com)

A numerical study has been made of laminar core-annular through a torus. It is a follow-up of the study by Picardo and Pushpavanam, AIChE J. 2013;59(12):4871–4886, who obtained an analytical solution for the case that the core is concentric and circular. In our study, we investigated the possibility of eccentric core-annular flow and the deformation of the core-annular interface. We found that a stable eccentric core position is possible, which is shifted in the direction of the inner or outer side of the torus depending on the balance of the normal stresses at the core-annular interface. When these stresses are too far off from those for concentric and circular core-annular flow, fouling of the wall occurs. We compared the results of core-annular flow in a torus with those for a 90° pipe bend and found that the flow pattern in the torus is representative for the flow pattern in the bend. © 2015 American Institute of Chemical Engineers *AIChE J*, 61: 2319–2328, 2015

Keywords: core-annular flow, torus, numerical simulation

Introduction

We study the flow of a high-viscosity liquid surrounded by a low-viscosity liquid through a pipe. This core-annular flow is very interesting from a practical and scientific point of view. Much attention has been paid in the literature to core-annular flow. Joseph and Renardy[1] have written a book about it. There are several review articles, see for instance Oliemans and Ooms[2] and Joseph et al.[3] A description of our recent research can be found in Ooms et al.[4] and Beerens et al.[5]

Most studies about core-annular flow have focused on straight vertical or horizontal pipes. There are not many studies on core-annular flow in a curved pipe. However, during pipeline transport of very viscous oil with water, one has to deal with curved parts in the pipeline. Moreover in microfluidic applications of core-annular flow 90° bends and 180° return bends are often used. Compared with core-annular flow in a straight pipe, the flow in a curved one is more complicated. The centrifugal force has a strong influence on the flow pattern, causing a secondary flow in a cross-section perpendicular to the torus pipe. Fouling of the pipe wall by the core liquid is more likely to occur than in a straight pipe. Therefore, we decided to study core-annular flow in a curved pipe in more detail.

In recent years, first experimental and numerical investigations of core-annular flow in a curved pipe have been performed. Sharma et al.[6] investigated the hydrodynamics of lube oil and water flow through a return bend connecting two horizontal pipes. They reported extensive measurements on two bend geometries (U-bend and rectangular bend). They observed that the bend geometry has a strong influence on the downstream phase distribution. (A similar study was performed by Sharma et al.[7] for a low-viscosity oil [kerosene] and water.) Ghosh et al.[8] reported a computational fluid dynamics (CFD) analysis (applying the volume-of-fluid [VOF] method) of core-annular flow of lube oil and water through a return bend. A satisfactory agreement was found between numerically obtained phase distributions and experiments reported by Sharma et al.[6] Jiang et al.[9] used (what they call) the Eulerian model to simulate core-annular flow through a U-bend. In their Eulerian model it was assumed that the core liquid and annular liquid formed two interpenetrating liquids with mutual interaction. The results of their calculations compared well with experimental observations and with numerical results based on the VOF method mentioned before. Jiang et al.[10] made a numerical study of core-annular flow through a II-bend using the VOF method. The influence of the input water fraction, oil properties, and geometric parameters on the hydrodynamic quantities and on the fouling characteristics was investigated. In all of the aforementioned studies the flow in the water was assumed to be turbulent. So in the numerical simulations a two-equation turbulence model (the k-ε model) was applied.

A different (original and interesting) approach to study core-annular flow in a curved pipe was made by Picardo and Pushpavanam.[11] They focused on the case of a fully developed laminar core-annular flow in a torus with a concentric, circular core. This problem was solved by them analytically and resulted in a detailed understanding of the prominent physical mechanisms governing the flow. The condition on the physical parameters for the core to be concentric and

Correspondence concerning this article should be addressed to G. Ooms at g.ooms@tudelft.nl.

circular was derived by accounting for the normal stresses at the core-annular interface. Two-key features of the flow, the secondary circulations and the redistribution of the axial velocity, were described in detail. The viscous coupling of the two liquids at the interface led to a variety of circulation patterns and axial profiles, depending on the system parameters. The parameter space was divided into different regions using analytical conditions at the transition between the flow regimes. They mentioned in their article, that the results and conclusion of their study of concentric core-annular flow in a torus can aid in future investigations of the more general problem in which the core is nonconcentric and noncircular.

We followed the suggestion of Picardo and Pushpavanam and studied (numerically) core-annular flow in a torus with an eccentric and noncircular core. We started by repeating one of their calculations to investigate whether we could reproduce their result and to find out whether the flow was stationary and stable. Then we changed the balance of the normal stresses at the core-annular interface by increasing or decreasing the interfacial tension. It is important to realize that in a torus the interface curvature at the inner and outer side of the torus is different, causing a net normal stress on the core in the radial direction. When the interfacial tension is increased or decreased, we expected the core to move away from its original position and become eccentric (and perhaps deformed). We also investigated the possibility of fouling of the torus wall by the core liquid. Next we repeated some of the calculations but with an initial wave at the core-annular interface and studied the wave development as a function of time.

Numerical Scheme

We solved numerically the Navier–Stokes equations for the flow in the core liquid and annular liquid. The chosen flow conditions were such that the flow in both liquids was laminar. So, no turbulence model has been used. Although no turbulence was present, the inertial forces played an important role. For our numerical analysis the package OpenFoam version 2.1.1 was used. To simulate the flow of two liquids (with different densities) the VOF method is an important numerical tool. We applied the interFoam solver in the package OpenFOAM which uses the VOF method. The VOF method has the advantage with respect to the Eulerian–Lagrangian approaches (which traces the interface and regrid if the position of the interface changes) that it is able to represent complicated changes in the interface, as it does not depend on regridding but can use a stationary grid.

A brief summary of the VOF method is given following the description given by Bohorquez.[12] The continuity equation is given by

$$\frac{\partial \rho}{\partial t}+\nabla\cdot(\rho\mathbf{v})=0 \tag{1}$$

in which the mixture density is given by

$$\rho=\rho_1\alpha+\rho_2(1-\alpha) \tag{2}$$

ρ_1 the density of the core liquid and ρ_2 the density of the annular liquid. $\mathbf{v}$ is the mass-average velocity

$$\mathbf{v}=\frac{1}{\rho}[\rho_1\alpha\mathbf{v}_1+\rho_2(1-\alpha)\mathbf{v}_2] \tag{3}$$

$\mathbf{v}_1$ and $\mathbf{v}_2$ are the conditionally averaged velocities of core liquid and annular liquid, respectively. The α-equation (VOF equation) is given by

$$\frac{\partial \alpha}{\partial t}+\nabla\cdot(\alpha\mathbf{u})+\nabla\cdot[\alpha(1-\alpha)\mathbf{u}_{r\alpha}]=0 \tag{4}$$

$\mathbf{u}$ is the volumetric velocity, which is related to the mass-average velocity in the following way

$$\mathbf{u}=\alpha\mathbf{v}_1+(1-\alpha)\mathbf{v}_2 \tag{5}$$

The relative velocity $\mathbf{u}_{r\alpha}$ is equal to

$$\mathbf{u}_{r\alpha}=\mathbf{v}_1-\mathbf{v}_2 \tag{6}$$

The equation of motion is

$$\frac{\partial \rho\mathbf{v}}{\partial t}+\nabla\cdot(\rho\mathbf{v}\mathbf{v})=\rho\mathbf{g}-\nabla p+\nabla\cdot(\tau^{(1)}+\tau^{(2)})-\gamma\kappa\nabla\alpha \tag{7}$$

where the mixture pressure is given by

$$p=p_1+p_2 \tag{8}$$

and the bulk laminar stress tensor $\tau^{(1)}$ by

$$\tau^{(1)}=\alpha\tau_1^{(1)}+(1-\alpha)\tau_2^{(1)} \tag{9}$$

in which $\tau_1^{(1)}$ and $\tau_2^{(1)}$ are the laminar stresses of the two individual phases. For a thin interface between the two-phases the mixture viscosity μ may be assumed to be given by

$$\mu=\mu_1\alpha+\mu_2(1-\alpha) \tag{10}$$

μ_1 the viscosity of the core liquid and μ_2 the viscosity of the annular liquid. The tensor $\tau^{(2)}$ represents the momentum diffusion due to the relative motion between the two-phases. It is therefore called the "diffusion stress term." (The details about the modeling of this term can be found in Bohorquez[12].) To model the effect of the surface tension the term $-\gamma\kappa\nabla\alpha$ is added to the right-hand side (RHS) of the momentum balance equation as suggested Brackbill et al.[13] γ is the interfacial tension and κ the local surface curvature. (Again for details see Bohorquez[12]). When there is no slip between the two-phases $\mathbf{u}_{r\alpha}=0$ and $\mathbf{u}=\mathbf{v}$.

OpenFoam applies the finite-volume method to solve the relevant partial differential equations. The Gauss limited linear V method was used for the advection terms of the velocity components and the Gauss van Leer method for the advection term of the scalar. For the pressure–velocity coupling the PIMPLE scheme was applied. PIMPLE is the merged PISO-SIMPLE (semi-implicit method for pressure-linked equations) scheme. The following linear solvers were used: Preconditioned Conjugate Gradient for the pressure and Preconditioned BiConjugate Gradient for the velocity components. The coarsest mesh that we applied in a cross-section of the torus is shown in Figure 1. We used a hexahedral grid, equidistant in axial flow direction. For the mesh shown in Figure 1 there are in radial direction 34 grid points (10 in the annulus and 24 ($10+20/2^{1/2}$) in the core), 80 grid points in circumferential direction and 100 grid points in axial direction. We also used a finer grid with 97, 160, and 100 grid points in radial, circumferential en axial direction, respectively. Our finest mesh had 195, 320, and 100 grid points. Like Picardo and Pushpavanam, we imposed a constant pressure gradient along the axial centerline of the torus. On the pipe wall the no-slip boundary condition was imposed. As initial conditions inside the pipe we used the analytical solution of Li and Renardy[14] for perfect core-annular flow in a straight pipe (on a local basis).

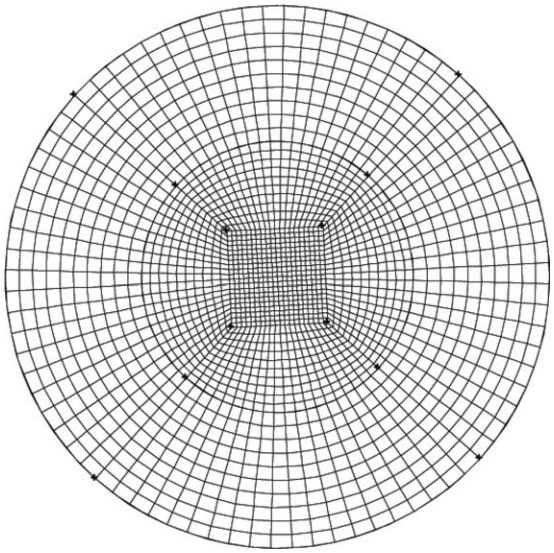

Figure 1. Coarsest mesh in a cross-section of the torus used in the calculation.

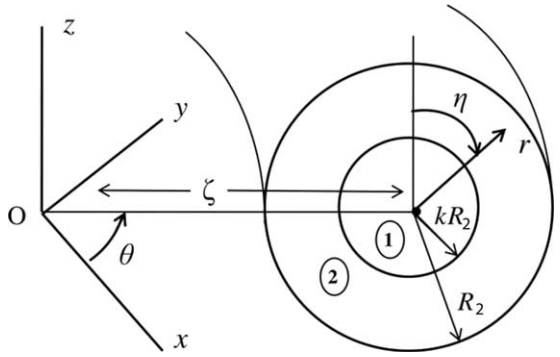

Figure 2. Orthogonal curvilinear coordinates.

Results

Comparison with one of the results of Picardo and Pushpavanam

Picardo and Pushpavanam made use of the orthogonal curvilinear coordinates (r, η, θ) shown in Figure 2. θ is the axial coordinate in the length direction of the torus, whereas r, η are the radial and circumferential coordinates in a normal cross-section of the torus. R_2 is the radius of the torus in a normal cross-section. The quantity $k=R_1/R_2$ in which R_1 is the radius of the core in a normal cross-section of the torus pipe. ζ is the radius of curvature of the total torus (see Figure 2). Picardo and Pushpavanam made the continuity equation and the equation of motion dimensionless and found the following dimensionless groups: the Reynolds numbers $\mathrm{Re}_1 = \rho_1 G R_2^3/\mu_1^2$, $\mathrm{Re}_2 = \rho_2 G R_2^3/\mu_2^2$, the viscosity ratio μ_1/μ_2, the fractional core radius $k=R_1/R_2$, the curvature ratio $\epsilon=R_2/\zeta$ and the capillary number $\mathrm{Ca}=GR_2^2/\gamma$. G is the constant pressure gradient imposed along the axial centerline of the torus ($G=\frac{1}{\zeta}\frac{\partial p}{\partial \theta}$). Picardo and Pushpavanam solved the dimensionless equations by means of a perturbation parameter with ϵ as the small parameter. So in zeroth-order approximation their problem reduced to core-annular flow in a straight pipe. The influence of the curvature was taken into account in their first-order calculation. They assumed that the core-annular interface is circular and concentric. This led to a relation between the dimensionless groups. For instance when Re_1, Re_2, μ_1/μ_2, and k are given, Ca can be determined from this relation. (We will return to this point in more detail later on.) The calculated flow fields showed a rich variety of secondary flows in a normal cross-section of the torus pipe with vortices in the core and the annulus. For instance, the core liquid can dominate (drive) the annular liquid or vice versa. They presented in their paper a circulatory flow regime map on the $(k, \frac{\mu_1}{\mu_2})$-plane at various values for Re_1 and Re_2. For the details we refer to the paper by Picardo and Pushpavanam.[11]

To check our calculations we selected one of the cases of Picardo and Pushpavanam for which the parameters have the following values: $\mathrm{Re}_1=30$, $\mathrm{Re}_2=30$, $\mu_1/\mu_2=1.9$, and $k=0.5$. We chose $\epsilon=1/6$. The circulatory flow pattern for this case is according to them given by Figure 3. As can be seen there is a pair of counter-rotating vortices in the core and in the annulus. Picardo and Pushpavanam call the vortices for this case principal vortices. As the flow on either side of the interface flows in opposite directions, the velocity must be identically zero at the interface. We performed a numerical simulation for this same case. To that purpose we chose the following values of the relevant quantities: $R_2=0.00476$ m (We used this value also in our earlier calculations. It is equal to the pipe radius used in the experiments by Bai et al.[15]). As $k=0.5$, $R_1=0.00238$ m. We chose $\mu_2=0.010$ kg/m s. As $\mu_1/\mu_2=1.9$, $\mu_1=0.019$ kg/m s. As $\epsilon=1/6$, $\zeta=0.02856$ m. We chose $\rho_1=1000$ kg/m^3. As $\mathrm{Re}_1=30$, $G=100.4$ kg/ms. As $\mathrm{Re}_2=30$, $\rho_2=277$ kg/m^3. From the relation between the dimensionless groups derived by Picardo and Pushpavanam, we find $\mathrm{Ca}=0.4555$. So $\gamma=0.005$ kg/s^2. For these values we performed our numerical simulation. (The boundary condition and initial condition have been discussed before.) The result for the distribution of the core liquid and annular liquid in a cross-section through the torus for $z=0$ is shown in Figure 4. As can be seen this distribution remains the same over 20 s. As the velocity of the core at the centerline is about $V_0=0.05$ m/s, the core has travelled a distance of about 1 m, which is about six times the torus length. During this time the core remains concentric as also found by Picardo and Pushpavanam. The cross-section remained perfectly circular (see

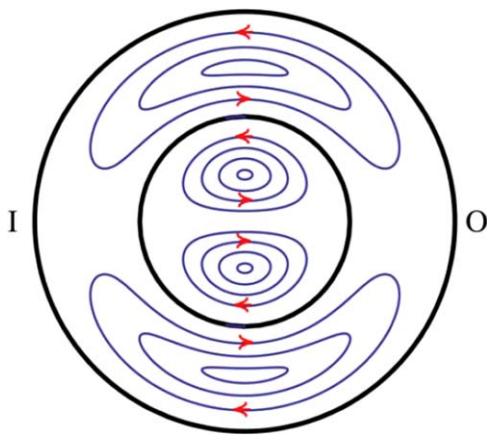

Figure 3. Secondary flows for the case $\mathrm{Re}_1=30$, $\mathrm{Re}_2=30$, $\mu_1/\mu_2=1.9$ and $k=0.5$ according to Picardo and Pushpavanam.[11] I indicates the inner side of the torus and O the outer side.

[Color figure can be viewed in the online issue, which is available at wileyonlinelibrary.com.]

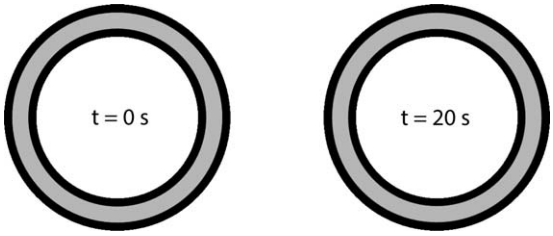

Figure 4. Cross-section through the torus for $z = 0$ for the case γ=0.005 kg/s^2.

Gray: core liquid; black: annular liquid.

Figure 5). No disturbances in the form of waves appear at the interface. So the flow remains stable. When we calculate the Reynolds numbers according to Li and Renardy[14] we find: $\mathrm{Re}_{1,\mathrm{LR}}=\rho_1 V_0 R_1/\mu_1=6.26$ and $\mathrm{Re}_{2,\mathrm{LR}}=\rho_2 V_0 R_1/\mu_2=3.29$. According to analytical stability calculations (see Joseph and Renardy[1]) core-annular flow in a straight pipe is indeed stable at these low values of the Reynolds numbers. So it seems that this holds also for a curved pipe.

The axial velocity distribution (in the θ-direction) of the (main) flow along a line in the z-direction ($\eta = 0$) through the torus center in a normal cross-section of the torus pipe is given in Figure 6. A vector plot of the secondary flow is given in Figure 7. (In this vector plot all vectors indicate the local flow direction. Their lengths are not representative for the magnitude of the local velocity.) The circumferential velocity distribution of the (secondary) flow along a line in the z-direction ($\eta = 0$) through the torus center in a normal cross-section of the torus pipe is shown in Figure 8.

Figures 6 and 8 show also the analytical results by Picardo and Pushpavanam. For the axial velocity distrtibution the agreement is perfect. Figure 8 shows a small difference between the analytical and numerical results for the circumferential velocity distribution in the core region of the flow. Small fluctuations (of about 10%) as a function of time remained in the circumferential velocity distribution (also for the finest grid and the highest accuracy with tolerance of 10^{-9} in the velocity calculation). In Figures 9 and 10 the relative error between the numerical and theoretical results are shown.

Figure 7 shows that there are three vortex pairs. Looking only at the top half semicircle of the cross-section, it is clear that there is one vortex in the core, one vortex near the wall and an additional vortex in-between them. This in-between vortex seems to be a sandwich vortex (as reported by Picardo and Pushpavanam). So it seems that there is some difference between the flow pattern calculated numerically and

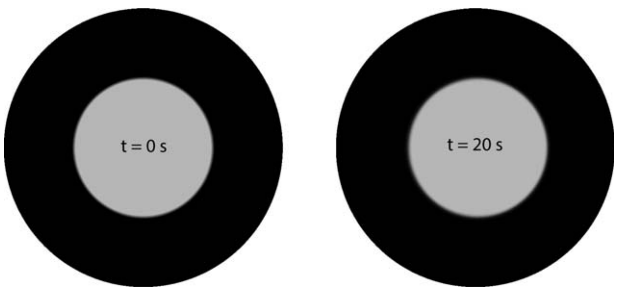

Figure 5. Normal cross-section of the torus pipe for the case γ=0.005 kg/s^2.

Gray: core liquid; black: annular liquid.

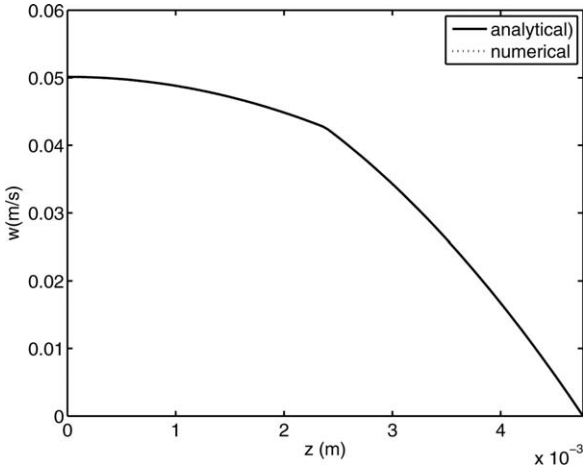

Figure 6. Axial velocity distribution of the (main) flow along a line in the z-direction ($\eta = 0$) through the torus center in a normal cross-section of the torus pipe for the case γ=0.005 kg/s^2. (See Figure 2 for an explanation of z, θ, and η.)

Perfect agreement between numerical and analytical result.

the analytical result shown in Figure 3. We suspect that this difference is due to the 10% fluctuation in the v-component of the cross-velocity mentioned above.

Changing the normal stress balance at the interface by increasing the interfacial tension

Picardo and Pushpavanam used the length scale R_2, the velocity scale GR_2^2/μ_i and the pressure scale GR_2 to write the continuity equation, equation of motion, and boundary conditions in a dimensionless manner. (The subscript i is an index which denotes the liquids; $i = 1$ denotes the core liquid

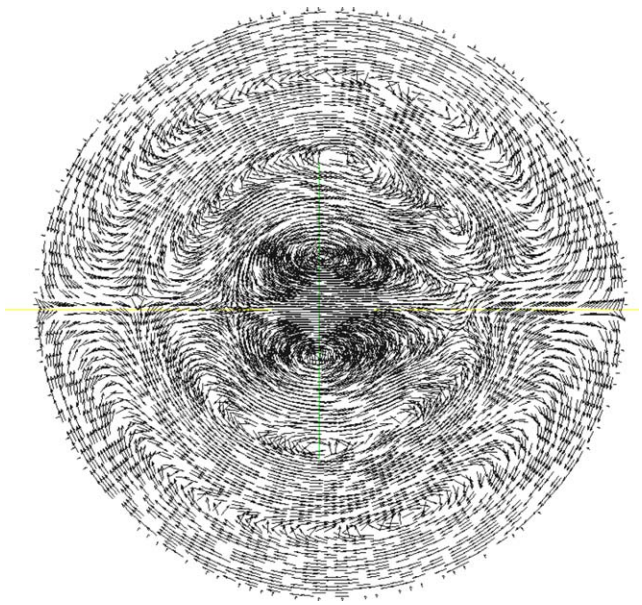

Figure 7. Secondary flows for the case γ=0.005 kg/s^2 according to our numerical calculation.

Left-hand side: inner side of the torus; right-hand side: outer side of the torus. [Color figure can be viewed in the online issue, which is available at wileyonlinelibrary.com.]

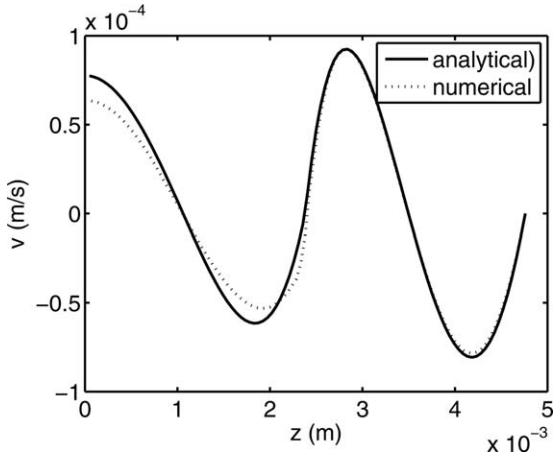

Figure 8. Circumferential velocity distribution of the (secondary) flow along a line in the *z*-direction ($\eta = 0$) through the torus center in a normal cross-section of the torus pipe for the case γ=0.005 kg/s^2.

and $i = 2$ the annular liquid.) As aforementioned they solved these equations analytically by means of a perturbation parameter with $\epsilon = R_2/\zeta$ as small parameter. The normal stress balance at the interface can in dimensionless form be written as

$$p_1 - p_2 + 2\left(\frac{\partial u_2}{\partial r} - \frac{\partial u_1}{\partial r}\right) = \frac{1}{\mathrm{Ca}}\left[\frac{1}{k} + \epsilon\frac{\sin\eta}{(1+\epsilon r\sin\eta)}\right] \qquad (11)$$

in which u_1 and u_2 are the radial velocity components in the core liquid and annular liquid respectively. p_1 and p_2 are the pressures. In zeroth-order approximation ($\in = 0$) this equation is the Young–Laplace equation and the pressure difference is independent of r and η. However, in first-order approximation the pressure jump becomes dependent on the radial and circumferential coordinates. As mentioned, Picardo and Pushpavanam solved the continuity equation and equation of motion satisfying the boundary conditions assuming the core to be concentric and circular. Substituting the calculated velocities and pressures in Eq. 11 they found a relation between *Ca* and the other dimensionless groups Re_1, Re_2, μ_1/μ_2, and k. So when these other dimensionless groups are given *Ca* is known. For the case presented in the preceding section this led to a value of the interfacial tension of γ=0.005 kg/s^2.

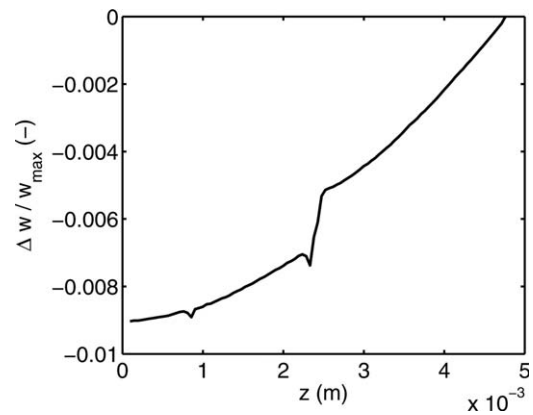

Figure 9. Relative error in the axial velocity distribution given in Figure 6.

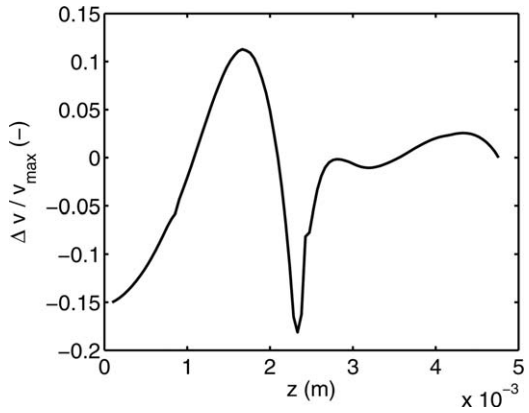

Figure 10. Relative error in the circumferential velocity distribution given in Figure 8.

In our study of eccentric core-annular flow we started from the flow pattern derived in the preceding section (with a concentric and circular core) and then changed the value of γ. We were interested to find out, whether steady core-annular flows were possible with an eccentric and deformed core. In our first calculation we changed the value of γ from 0.005 to 0.006 kg/s^2 and followed the development of the flow as a function of time. The result for the core position and for the core deformation is shown in Figure 11. As can

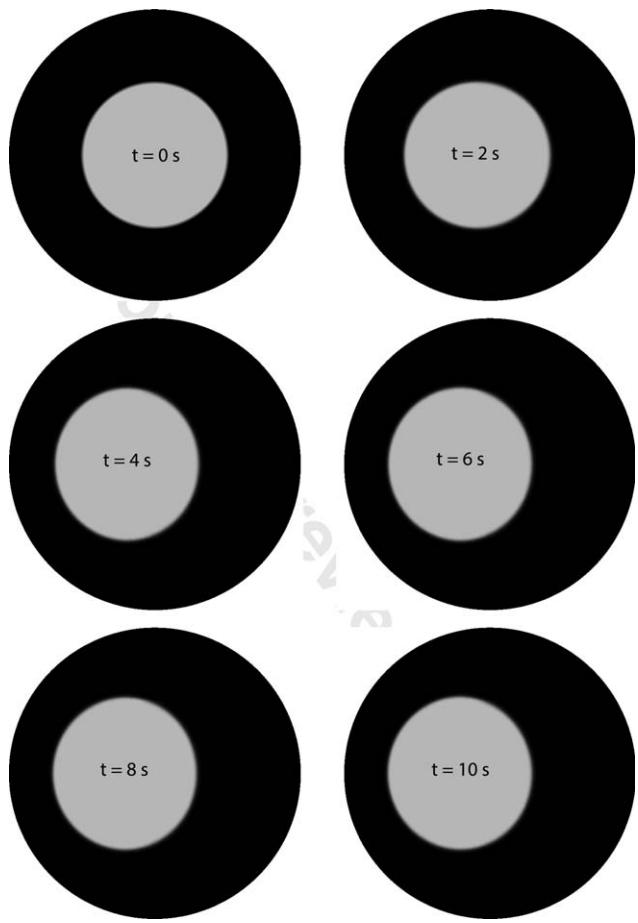

Figure 11. Normal cross-section of the torus for the case γ=0.006 kg/s^2.

Gray: core liquid; black: annular liquid. Left-hand side: inner side of the torus; right-hand side: outer side of the torus.

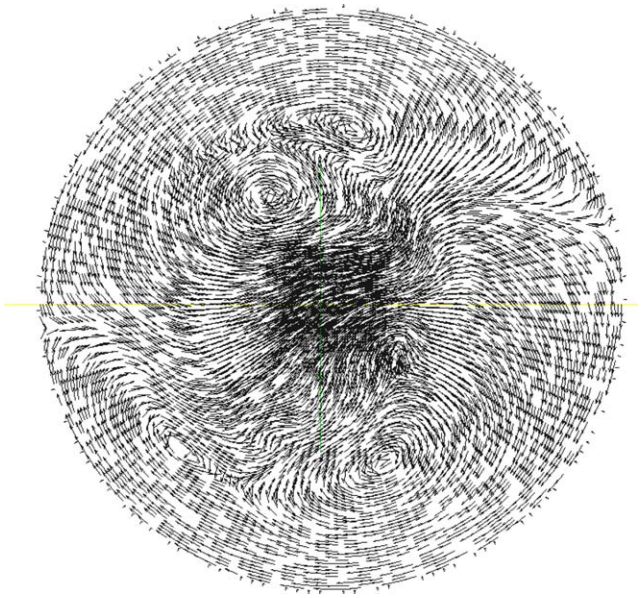

Figure 12. Vector plot of the secondary flow for the case γ=0.006 kg/s^2 at t=10 s.

Left-hand side: inner side of the torus; right-hand side: outer side of the torus. [Color figure can be viewed in the online issue, which is available at wileyonlinelibrary.com.]

be seen the core started at t=0 s to move from the torus center to the inner side of the torus and reached its new stationary state at around t=6 s. During that period the core shape changed slightly from a circular to an ellipsoidal shape. After t=6 s the core was again stable; no waves developed at the interface. The secondary flow in a normal cross-section of the torus is given in Figure 12. The circumferential velocity distribution of the secondary flow along a line in the z-direction ($\eta = 0$) through the torus center in a normal cross-section of the torus pipe is shown in Figure 13. These figures show that the flow pattern has changed considerably from the pattern for concentric core-annular flow given in Figure 7.

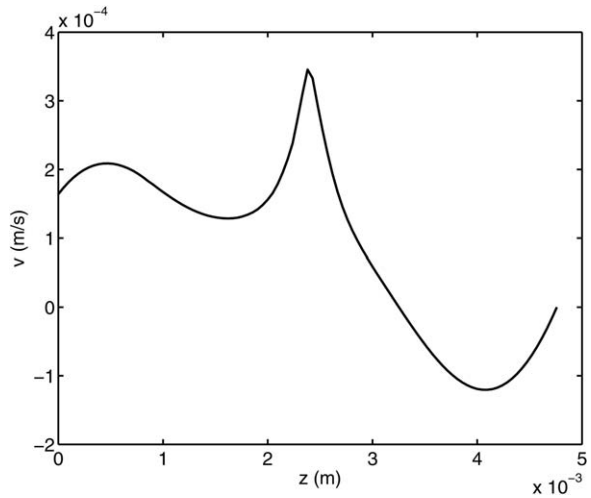

Figure 13. Circumferential velocity distribution of the (secondary) flow along a line in the z-direction ($\eta = 0$) through the torus center in a normal cross-section of the torus pipe for the case γ=0.006 kg/s^2.

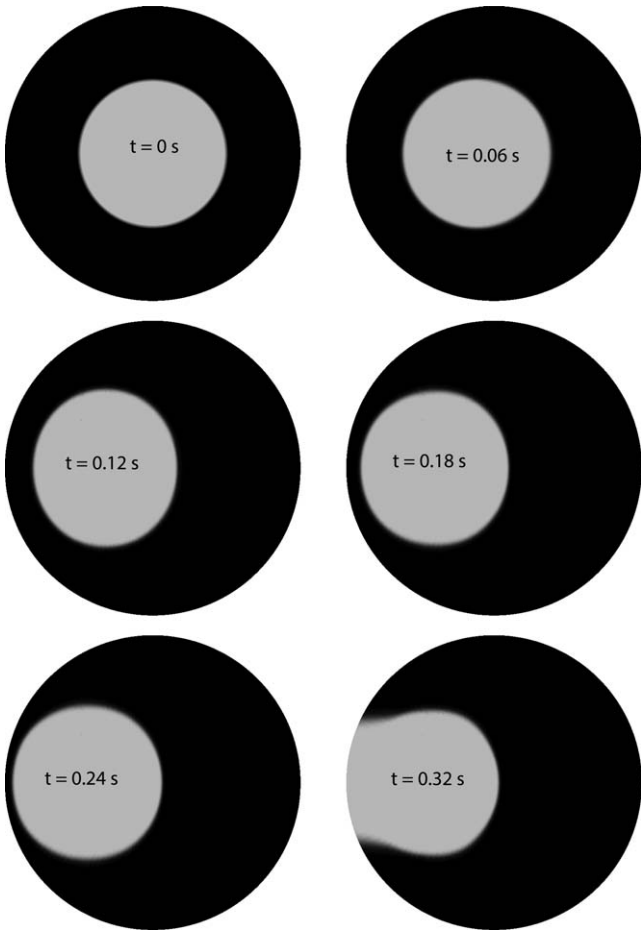

Figure 14. Normal cross-section of the torus for the case γ=0.100 kg/s^2.

Gray: core liquid; black: annular liquid. Left-hand side: inner side of the torus; right-hand side: outer side of the torus.

Next we started again from the flow pattern derived in the preceding section (with a concentric and circular core) and then changed the value of γ from 0.005 to 0.100 kg/s^2. This change had a very strong effect on the flow. As can be seen in Figure 14 the core moved quickly to the inner side of the torus and touched and fouled the wall at around t=0.3 s. Obviously the balance of the normal stresses at interface had changed so drastically due to the strong increase of the interfacial tension, that an equilibrium position was no longer possible.

Changing the normal stress at the interface by decreasing the interfacial tension

In the subsequent step of our study, we started again from the flow pattern with a concentric and circular core and then changed the value of γ from 0.005 to 0.004 kg/s^2. The result for the core position is given in Figure 15. In this case, the core moved to the outer side of the torus, while its shape changed slightly. At about t=6 s the core was at its stationary position and remained stable. We continued this computation for a long time, up to t = 16.5 s. A small disturbance occurred at the interface which moves around the torus. It did not grow and foul the wall. In Figure 16, a cross-section of the total torus for z=0 m is given. The disturbance of the interface is hardly visible. A vector plot of

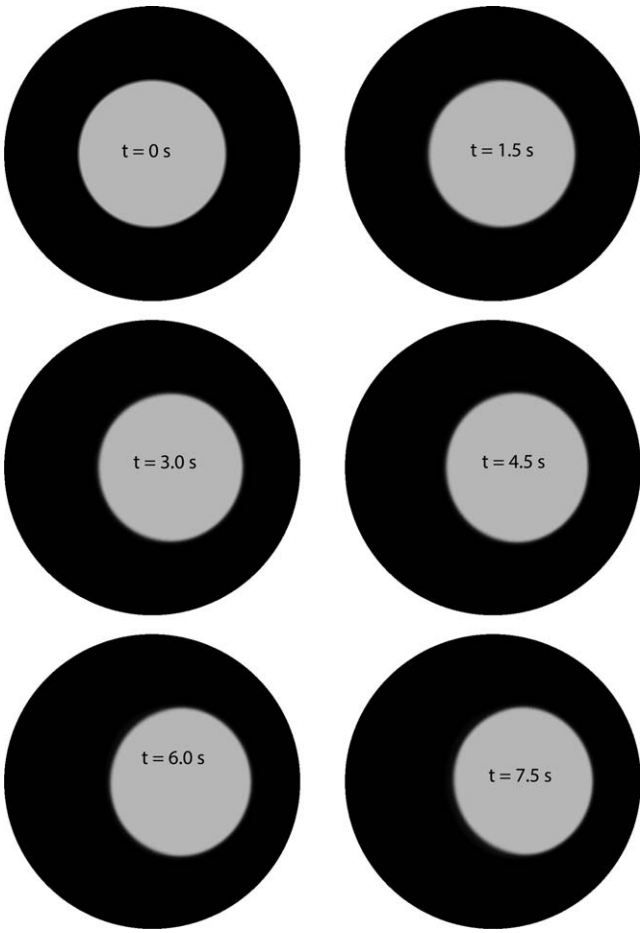

Figure 15. Normal cross-section of the torus for the case γ=0.004 kg/s^2.

Gray: core liquid; black: annular liquid. Left-hand side: inner side of the torus; right-hand side: outer side of the torus.

the secondary flow for $t = 16.5$ s is shown in Figure 17. The circumferential velocity distribution of the (secondary) flow along a line in the z-direction ($\eta = 0$) through the torus center in a normal cross-section of the torus pipe for $t = 16.5$ s is shown in Figure 18.

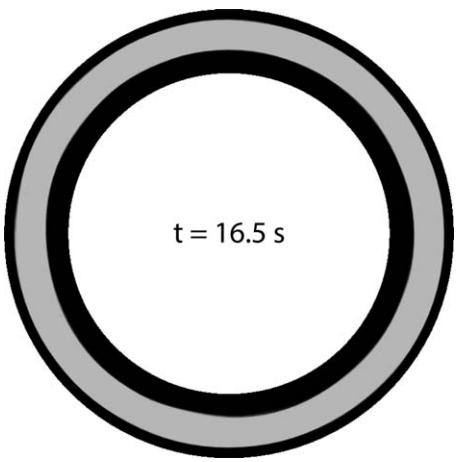

Figure 16. Cross-section through the torus for $z = 0$ for the case γ=0.004 kg/s^2.

Gray: core liquid; black: annular liquid.

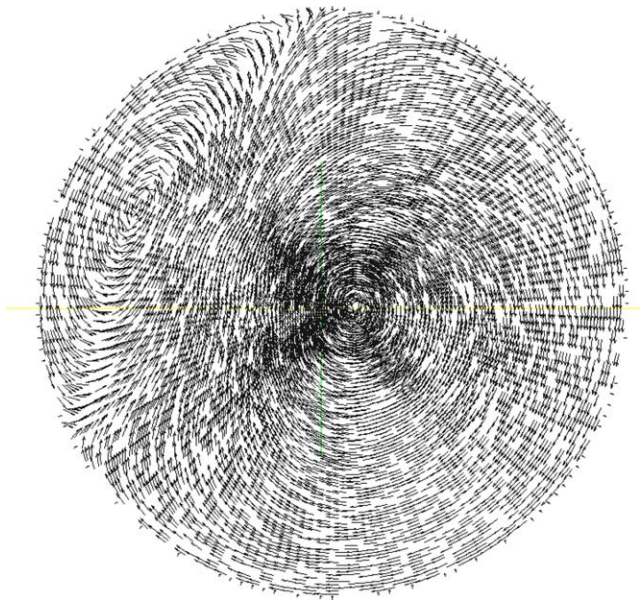

Figure 17. Secondary flow for the case γ=0.004 kg/s^2 according to our numerical calculation.

[Color figure can be viewed in the online issue, which is available at wileyonlinelibrary.com.]

Next, we repeated this calculation, but now for a value of the interfacial tension of 0.001 kg/s^2. The result of the core position and shape is shown in Figure 19. This time the core seemed to become stationary at a small distance from the torus wall. Even at t=12 s the core did not touch the wall. We continued the calculation and found, however, that between t=12 s and t=15 s fouling occurred. The late fouling in this case is perhaps due to the lower value of the interfacial tension, which makes it possible that the core-annular interface adapts more easily to the flow and stays away from the wall for a longer time.

We always checked the convergence of the computations by calculating the total radial momentum of the core as a function of time. As an example we show the result for the case γ=0.001 kg/s^2 in Figure 20. As can be seen the core

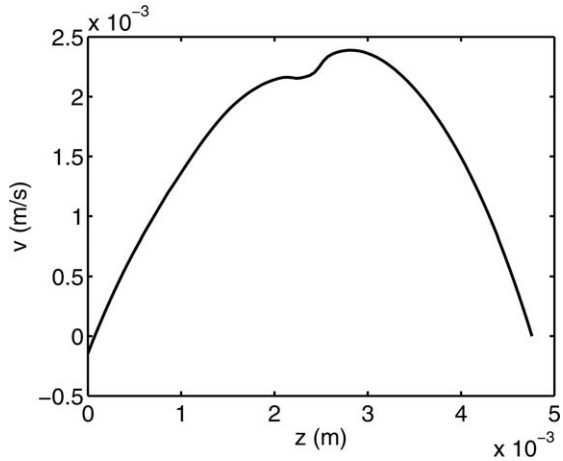

Figure 18. Circumferential velocity distribution of the (secondary) flow along a line in the z-direction ($\eta = 0$) through the torus center in a normal cross-section of the torus pipe for the case γ=0.004 kg/s^2.

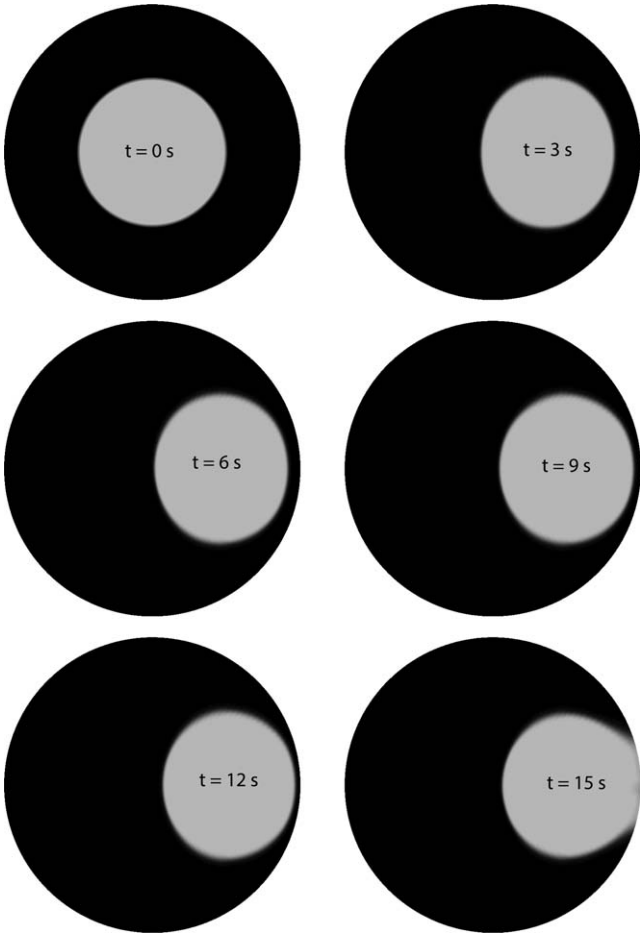

Figure 19. Normal cross-section of the torus for the case γ=0.001 kg/s^2.

Gray: core liquid; black: annular liquid. Left-hand side: inner side of the torus; right-hand side: outer side of the torus.

started to move after t=0 s in radial direction, the total radial momentum reached a maximum and then decreased again to zero. However, between t=12 and t=15 s there is a new peak in the momentum caused by the fouling of the wall.

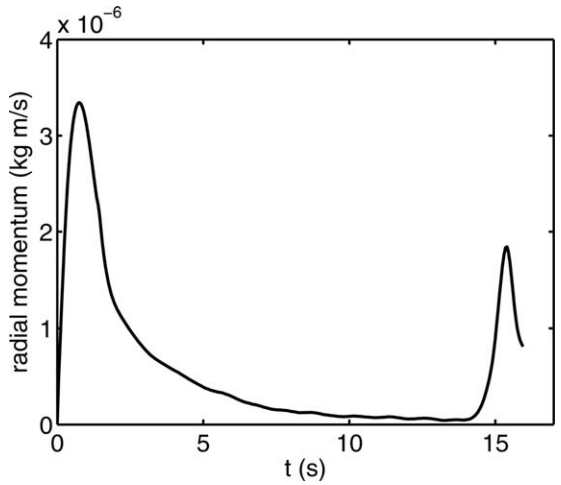

Figure 20. Total radial momentum of the torus as a function of time for the case γ=0.001 kg/s^2.

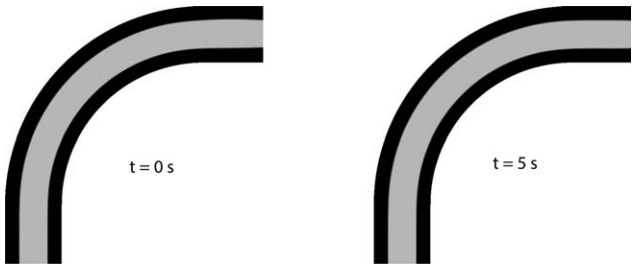

Figure 21. Core-annular flow in a 90° bend for the chosen case of Picardo and Pushpavanam (with γ=0.005 kg/s^2).

Applying the Picardo-and-Pushpavanam case (with γ=0.005 kg/s^2) to a 90° bend.

The study of core-annular flow in a torus is important from a scientific point of view. From a practical point of view core-annular flow in, for instance, a 90° bend is more interesting. As a side step in our research we applied, therefore, the Picardo-and-Pushpavanam case with γ=0.005 kg/s^2 to a 90° bend. The configuration is shown in Figure 21. So the curved part of the bend had the same curvature as the torus in the Picardo-and-Pushpavanam case. Also all other physical parameters were the same. Two parts of straight pipe were added to the inlet and outlet of the bend. At the inflow cross-section of the pipe the analytical solution of Li and Renardy[14] for perfect core-annular flow in a straight pipe was applied. At the outflow cross-section a zero velocity gradient and a fixed value for the (reduced) pressure was imposed. On the pipe wall the no-slip boundary condition was applied. As initial conditions inside the pipe we used again the analytical solution of Li and Renardy for perfect core-annular flow in a straight pipe (on a local basis). The result for the distribution of core liquid and annular liquid is given in Figure 21 at the start of the calculation (t=0 s) and at the end (t=5 s). As can be seen the distribution of the two liquids remained the same. The core stayed concentric and circular, like for the Picardo-and-Pushpavanam case. So the flow pattern for the torus is representative for the flow pattern in the 90° bend.

Numerical simulations for the Li-and-Renardy case

We have performed an additional torus calculation but this time for different values of the physical parameters. In this way, we checked whether the same conclusions could be drawn as those based on calculations with the physical parameters used in the preceding sections. For the new calculation we chose the physical parameters as applied by Li and Renardy (for core-annular flow in a straight pipe) and as used in our earlier calculations (see Ooms et al.[4] and Beerens et al.[5]). The physical parameters are given by μ_1=0.601, μ_2=0.001 kg/ms, ρ_1=905, ρ_2=995 kg/m^3, R_1=0.00372, R_2=0.00476 m, γ=8.54 · 10^{-3} kg/s^2, and G=150 kg/m^{2}s^2. For these values of the physical parameters the centerline velocity for smooth core-annular flow in a straight pipe is V_0=0.330 m/s. The torus curvature was kept the same (ϵ= 1/6) as for the Picardo-and-Pushpavanam case. The other dimensionless groups have the following values: Re$_1$= 4.05· 10^{-2}, Re$_2$= 1.609 · 10^4, k= 0.708, and μ_1/μ_2= 601. When we calculate the Reynolds numbers according to Li and Renardy[14] we find: Re$_{1,LR}$=$\rho_1 V_0 R_1/\mu_1$=1.848 and Re$_{2,LR}$=$\rho_2 V_0 R_1/\mu_2$= 1.221 · 10^3. The values of the physical parameters as used by

Li and Renardy come from the experiments by Bai et al.[15] During these experiments the flow in the annulus remained laminar.

First, we wanted to check whether the relation between the dimensionless groups as derived by Picaro and Pushpavanam for concentric and circular core-annular flow, was also valid for the Li-and-Renardy case. Using this relation we found the following value for the interfacial tension $\gamma = 0.28\,\mathrm{kg/s^2}$. So our calculations for this case were made with this value (so $\gamma = 0.28$ and not $\gamma = 8.54 \cdot 10^{-3}\ \mathrm{kg/s^2}$) to check, whether indeed the core remained concentric and circular as a function of time. The result is given in Figure 22. As can be seen the core remained indeed concentric and circular. After $t = 3\,\mathrm{s}$ the core was still in the same position. As the velocity of the core at the centerline was about $V_0 = 0.330\ \mathrm{m/s}$, the core had travelled a distance of about 1 m, which was about six times the torus length.

Next we studied the stability of the flow. We imposed a wave at the core-annular interface and studied the development of that wave. The result can be seen in Figure 23. The wave disappeared quickly, showing that core-annular flow was stable for the applied values of the physical parameters.

Discussion

Picardo and Pushpavanam derived theoretically a solution for concentric (circular) core-annular flow in a torus. Their analysis revealed several new interesting hydrodynamic phenomena. A striking result is the possible reversal of the circulation within either liquid. In single-phase flow liquid is transported from the inner side of the torus to the outer side along the centerline of the cross-section and then back to the inner side along the wall of the torus. Picardo and Pushpavanam found that (dependent on the values of the physical parameters) in core-annular flow it is possible that one of the liquids may influence the circulations in the other liquid and reverse the orientation of its vortices. This is not possible in single-phase flow.

We have checked numerically one of the cases of Picardo and Pushpavanam: the one with the two principal vortices (as they call them). We confirmed that indeed the flow was concentric and circular for that case. Moreover, we found that it is stationary and stable with respect to small disturbances. Thereafter, we investigated the sensitivity of the solution with respect to changes in the balance of the normal stresses at the core-annular interface. It turned out that with increasing values of the interfacial tension the core moved to the inner side of the torus. When the increase of the interfacial tension was not too large, a new eccentric stationary position was reached. When the interfacial tension became too large, the core touched and fouled the torus wall. With decreasing value of the interfacial tension the core moved to the outer side of the torus. It deformed and reached a new stationary position. Again: when the interfacial tension became too small, fouling occurred.

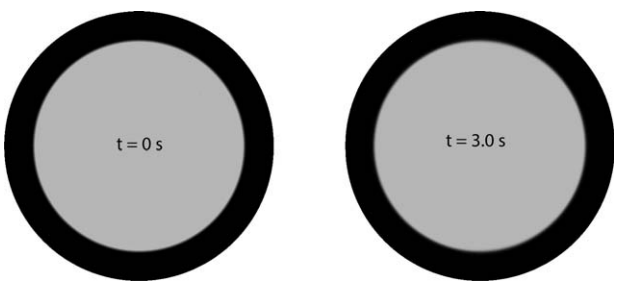

Figure 22. Li and Renardy case for concentric core-annular flow (with $\gamma = 0.28\,\mathrm{kg/s^2}$).

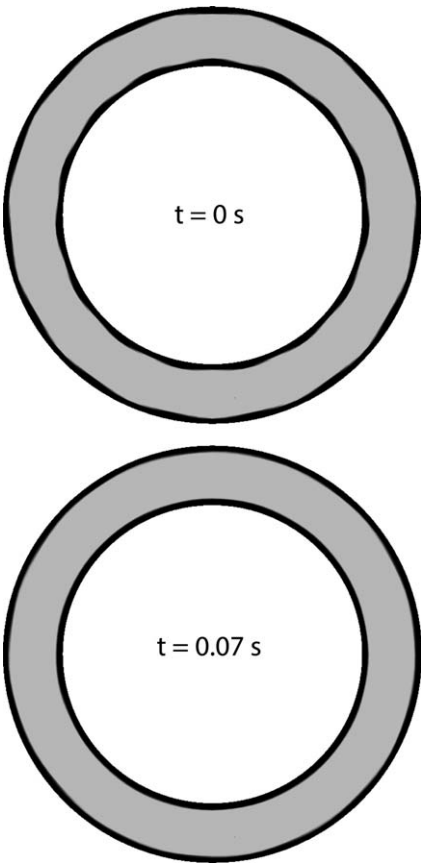

Figure 23. Influence of interfacial waves on the Li and Renardy case. Cross-section through the torus for $z = 0$ for the case $\gamma = 0.28\,\mathrm{kg/s^2}$.

It is interesting to study in our future work core-annular flow in a torus, when the torus curvature is no longer small. Such a study is difficult to carry out analytically. However, numerically that is very well possible. Also attention will be paid to the other cases found by Picardo and Pushpavanam; not the case with the two principal vortices, but cases with more complicated flow patterns. Attention must also be given to the buoyancy effect due to the difference in density of the two liquids.

Finally, we point out that with the open-source software OpenFoam it is very well possible to study the stability of flows, as shown in the calculation of the formation or suppression of waves at the core-annular interface reported, respectively, by Ooms et al.[4] and in this article. There are several articles in the literature that support this statement. For instance Cano-Lozano et al.[16] studied numerically (using OpenFoam) the transition from straight to zigzag motion during the rising of a single bubble in a still lquid. Gomez et al.[17] used the code to investigate the stability of the three-dimensional lid-driven cavity.

Literature Cited

1. Joseph DD, Renardy YY. *Fundamentals of Two-Fluid Dynamics, Part II: Lubricated Transport, Drops and Miscible Liquids*. New York: Springer-Verlag, 1993.

2. Oliemans RVA, Ooms G. Core-annular flow of oil and water through a pipeline. In: G.F. Hewitt, J.M. Delhaye, N. Zuber, editors. *Multiphase Science and Technology*. Washington: Hemisphere, 1986.
3. Joseph DD, Bai R, Chen KP, Renardy YY. Core-annular flows. *Ann Rev Fluid Mech*. 1991;29:65–90.
4. Ooms G, Pourquie MJBM, Beerens JC. On the levitation force in horizontal core-annular flow with a large viscosity ratio and small density ratio. *Phys Fluids*. 2013;25:32102.
5. Beerens JC, Ooms G, Pourquie MJBM, Westerweel J. A comparison between numerical predictions and theoretical and experimental results for laminar core-annular flow, *AIChE J*. 2014;60(8):3046–3056.
6. Sharma M, Ravi P, Ghosh S, Das G, Das PK. Hydrodynamics of lube oil-water flow through 180° return bends. *Chem Eng Sci*. 2011; 66:4468–4476.
7. Sharma M, Ravi P, Ghosh S, Das G, Das PK. Studies on low viscous oil-water flow through return bends. *Exp Therm Fluid Sci*. 2011;35:455–469.
8. Ghosh S, Das G, Das PK. Simulation of core annular flow in return bends-A comprehensive CFD study. *Chem Eng Res Des*. 2011;89: 2244–2253.
9. Jiang F, Wang Y, Ou J, Chen C. Numerical simulation of oil-water core annular flow in a U-bend based on the Eulerian model. *Chem Eng Techn*. 2014;37(4):659–666.
10. Jiang F, Wang Y, Ou J, Xiao Z. Numerical simulation on oil-water annular flow through the II bend. *Ind Eng Chem Res*. 2014;53:8235–8244.
11. Picardo JR, Pushpavanam S. Core-annular flow in a gently curved circular channel. *AIChE J*. 2013;59(12):4871–4886.
12. Bohorquez P. Finite volume method for falling liquid films carrying monodisperse spheres in Newtonian regime. *AIChE J*. 2012;58(8): 2601–2616.
13. Brackbill JU, Kothe DB, Zemach C. A continuum method for modeling surface tension. *J Comput Phys*. 1992;100:335–354.
14. Li J, Renardy YY. Direct simulation of unsteady axisymmetric core-annular flow with high viscosity ratio. *J Fluid Mech*. 1999;391:123–149.
15. Bai R, Chen K, Joseph DD. Lubricated pipelining: stability of core-annular flow. Part 5. Experiments and comparison with theory. *J Fluid Mech*. 1992;240:97–132.
16. Cano-Lozano JC, Bohorquez P, Martinez-Bazan C. Wake instability of a fixed axisymmetric bubble of realistic shape. *Int J Multiphase Flow*. 2013;51:11–21.
17. Gomez F, Gomez R, Theofilis V. On three-dimensional global linear instability analysis of flows with standard aerodynamic codes. *Aerosp Sci Technol*. 2014;32:223–234.

Manuscript received Jan. 27, 2015, and revision received Mar. 2, 2015.